Visualization Study of Counterflow in Superfluid ^{4}He using Metastable Helium Molecules

W. Guo, S.B. Cahn, J.A. Nikkel, W.F. Vinen and D.N. McKinsey

Xin Wen

Department of Physics and Astronomy, University of Tennessee, Knoxville

Neutron Scattering Division, Oak Ridge National Laboratory

Introduction

^{4}He has two liquid phases: He I, which is normal fluid and He II, the mix of normal fluid component and superfluid component (0 viscosity). When fluid flows in parallel with no disruption between the layers, the motion of the fluid is called laminar flow. The velocity of the fluid is constant at any point in the laminar flow. Another type of motion of fluid is turbulent flow. Turbulent flow is irregular flow that is characterized by chaotic changes in pressure and flow velocity. The velocity of this fluid is not constant at every point. The onset of turbulent flow depends on the fluids velocity, viscosity, density, and the size of the obstacle it encounters.

Heat is transferred in superfluid ^{4}He via a process known as thermal counterflow. In a thermal counterflow, the normal-fluid velocity v_n is related to the heat flux q by

$$q = \rho S T v_n \tag{1}$$

where ρ is the total density and S is the entropy per unit mass [1].

It has been known for many years that above a critical heat current the superfluid component in this counterflow becomes turbulent. It has been suspected that the normal-fluid component may become turbulent as well, but experimental verification is difficult without a technique for visualizing the flow. Here we report a series of visualization studies on the normal-fluid component in a thermal counterflow performed by imaging the motion of seeded metastable helium molecules using a laser-induced-fluorescence technique. This research presents evidence that the flow of the normal fluid is indeed turbulent at relatively large velocities. Thermal counterflow in which both components are turbulent presents us with a theoretically challenging type of turbulent behavior that is new to physics.

Previous techniques for visualization of thermal counterflow include particle image velocimetry [2] and particle tracking techniques [3]. They use micron-sized tracer particles formed from polymer spheres or solid hydrogen, ^{3}He or cluster of electrons as tracers to visualize thermal counterflow. These tracers can have limits. For example, micron-sized tracer particles can be trapped on the quantized vortex lines. Cluster of electrons repel each other and interact strongly with quantized vortices. Dr. Guo's group has demonstrated that metastable He_2* triplet molecules, with a radiative lifetime of about 13 s in liquid helium [4], can be imaged by using a laser-induced-fluorescence technique [5–8]. Metastable He_2* triplet molecules (~1 nm) won't be trapped by vortices above 1K [9]. Scattering by vortices has negligible effect. Thus, metastable He_2* triplet molecules have great potential to be the new tracer for thermal counterflow.

Results

The apparatus of the experiment is shown in Fig. 1. By applying a negative voltage to the needles (>emission threshold ~-500V), metastable helium molecules are produced near the needle apexes. If you generate a counterflow in the channel with the heater and metastable helium molecules will drift down with the flow. A focused pump laser pulse is used (910 nm) to drive the He_2 molecules along the beam path into the first vibrational level of the triplet ground electronic state. At a given delay time, an expanded probe laser pulse (925 nm) images selectively the vibrationally excited line of molecules by driving them to an excited electronic state and inducing 640 nm fluorescent light . Then an intensified CCD camera can be used to record the fluorescent light from the line of excited molecules.

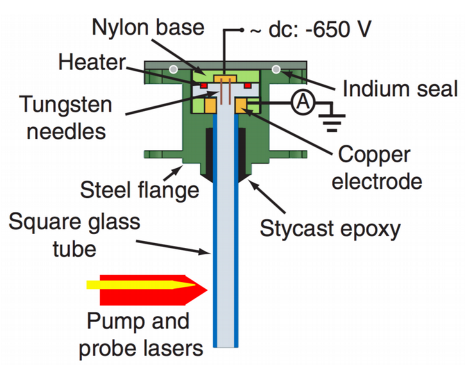

FIG. 1 Schematic diagram of the counterflow channel used in the molecule tagging experiment.

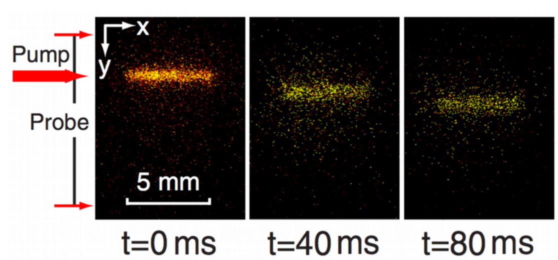

FIG. 2 Typical fluorescent images of a line of helium molecules taken at a heat flux of 640 mW/cm^2 and pump-probe delays of 0, 40, and 80 ms, respectively.

From Fig. 2, we can see that the straight line of molecules remains straight, indicating a flat normal-fluid velocity profile across the channel. Integrating the fluorescent signal in each pixel along the x-axis for each y value and doing a Lorentzian fit to the data, Fig. 3, we can say that the position of the molecule line is at x_0 (x_0 is its maximum). Then we can calculate the normal-fluid velocity. The results is shown in Fig. 4 does not include small heat flux data. This is because at small heat flux, metastable He_2* triplet molecules decay before they reach the laser area. The result agrees well with the prediction given by Eq (1) well.

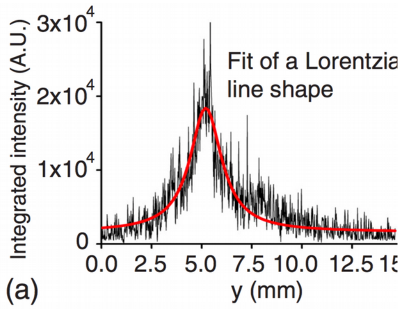

FIG. 3 A typical integrated cross-section profile of a molecule line in arbitrary units. The red line is a Lorentzian fit to the data.

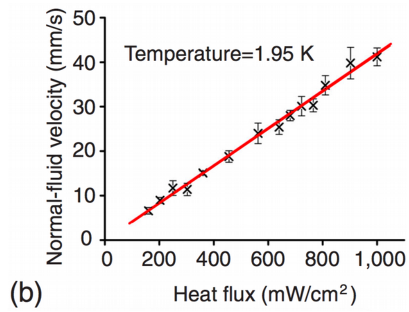

FIG. 4 The obtained normal-fluid velocity as a function of heat flux at 1.95 K

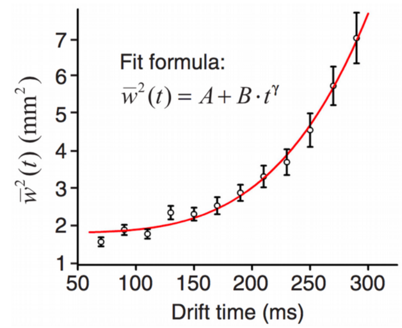

FIG. 5 The square of the width of a molecule line $\acute{w}^2(t)$ as a function of drift time t at a heat flux of 277 mW/cm^2

The molecule line width $\acute{w}(t)$ is defined to be the width of the peak at half maximum. The molecule line increase with time as shown in Fig. 5. The broadening of the molecule line is too rapidly to be explained by ordinary diffusion at experimental temperature 1.95K, meaning the flat velocity profile is caused by turbulent diffusion and the flow of normal fluid is turbulent. [10]

The normal-fluid velocity at small heat fluxes can be measured using a cluster tracking technique. The apparatus is shown in Fig. 8. First, apply a negative voltage pulse to the cathode and a small cluster of helium molecules is created near its apex with an initial diameter of 0.5-0.8 nm. Then, apply is a laser pulse (905 nm 500 Hz) that can drive the molecules to produce fluorescent light through a cycling transition. Fig. 7. The normal-fluid velocity can be measured and plotted in the same way as before.

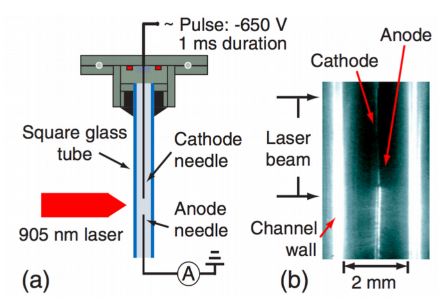

FIG. 6 (a) Schematic diagram of the counterflow channel used in the cluster tracking experiment. (b) An image of the square glass tube. A pulsed laser at 905 nm illuminates the needle apexes at about 2 cm from the open end of the channel.

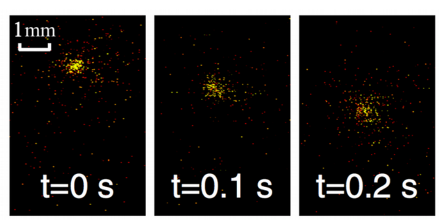

FIG. 7 Typical fluorescent images of a cluster of helium molecules taken at 0, 0.1, and 0.2 s after the cluster was created. The heat flux is 119 mW/cm^2. The temperature is 1.80 K. The exposure time for each image is 20 ms.

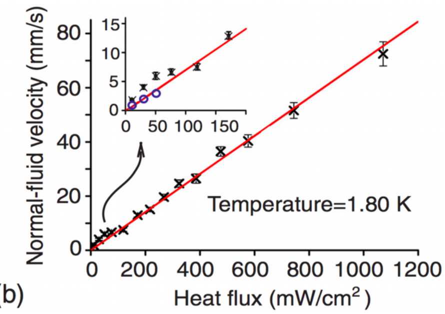

(b)

FIG. 8 The obtained normal-fluid velocity as a function of heat flux at 1.80 K. The black crosses are the data. The red line shows the calculated normal-fluid velocity based on Eq. (1) in the text. The blue circles in the inset for the small heat flux regime show the corresponding measured normal-fluid velocity divided by a factor of 2.

The results show a transition heat flux at about 50 mW/cm^2, which may correspond to the onset of quantum turbulence. It is likely that, in the small heat flux regime, both the superfluid and the normal fluid are in a laminar flow state. The drift velocity of the cluster should be twice the velocity given by Eq. (1) due to a Poiseuille profile [1] of the normal fluid [11]. This agrees with the result in Fig. 8.

Future Work

We believe that neutron beams enable measurements of turbulent flow under extreme conditions. Our current work is to demonstrate particle tracking velocimetry (PTV) using neutron beams to create metastable He_2* molecules at Oak Ridge National Laboratory. Once we prove the validity of this method, we will apply the technique to map turbulent flow about systematically fabricated models and compare results to models of turbulent flow. Our vision is to demonstrate an innovative capability to observe turbulent flow for applications in industry and science.

[1] L. D. Landau and E. M. Lifshitz, Fluid Mechanics (Pergamon Press, Oxford, 1987).

[2] S.W. Van Sciver, S. Fuzier, and T. Xu, J. Low Temp. Phys.148, 225 (2007).

[3] M. S. Paoletti et al., J. Phys. Soc. Jpn. 77, 111007 (2008).

[4] D. N. McKinsey et al., Phys. Rev. A 59, 200 (1999).

[5] D. N. McKinsey et al., Phys. Rev. Lett. 95, 111101 (2005).

[6] W. G. Rellergert et al., Phys. Rev. Lett. 100, 025301 (2008).

[7] W. Guo et al., Phys. Rev. Lett. 102, 235301 (2009).

[8] W. Guo et al., J. Low Temp. Phys. 158, 346 (2010).

[9] W. F. Vinen, Progress in Low Temperature Physics, AIP Conf. Proc. No. 850 (AIP, New York, 2006), p. 169.

[10] G. K. Batchelor, Proc. Cambridge Philos. Soc. 48, 345 (1952).

[11] M. Spiga and G. L. Morini, Int. Commun. Heat Mass Transf. 21, 469 (1994).